



Tectonic setting of the northwestern andes Constrained by a high-resolution earthquake catalog: Block Kinematics

Daniel Martínez-Jaramillo^{a,*}, Germán A. Prieto^b

^a Posgrado en Ciencias de la Tierra, Centro de Geociencias, Universidad Nacional Autónoma de México, Querétaro, Mexico

^b Departamento de Geociencias, Universidad Nacional de Colombia, Bogotá, Colombia

ARTICLE INFO

Keywords:

Uramite fault zone
Murindó fault
Murindó seismic cluster
Murindó earthquake
Mutatá earthquake
Panamá-chocó block

ABSTRACT

A high-precision earthquake catalog was generated using source-specific station terms and waveform cross-correlation techniques. This detailed catalog serves to interpret the crustal structure and deformation related to the tectonic setting in Northwestern South America. The Panamá-Chocó Block (PCB) is in contact with the Northwestern Andes causing crustal deformation and hence, fault interaction in the brittle regime leading to a high earthquake production concentrated in the Murindó Seismic Cluster (MSC) which is located in the north-eastern corner of the PCB. Slip on the Uramita Fault Zone (UFZ) is a response to the accommodation of the PCB against the North Andean block (NAB), splitting the fault into two segments, marked by an abrupt change in its strike. The north segment of the UFZ, a dextral transform fault (strike = S52°E and near vertical plane), which produced the Mutatá earthquake (2016-09-14, Mw = 6.2). The central segment of the UFZ strikes N12°E and exhibits mainly reverse slip with a subvertical fault plane which produced the 1987-03-19 Mw = 5.4 and 1987-11-11 Mw = 5.3 events. The Murindó sinistral strike-slip fault (strike = N9°W), which produced the great Murindó earthquake (1992-10-18, Mw = 7.1, epicentral intensity XI) is characterized by its wide zone of brittle deformation as a response to internal deformation of the PCB under a compressional NW-SE stress. Intermediate depth earthquakes are widely observed in the area, where we find evidence of the Caribbean slab subducting southwards beneath Panamá. The subduction of the Malpelo microplate to the south, shows high productivity within the Cauca Cluster and the presence of at least three finger-shaped mantle zones of seismicity.

1. Introduction

The western edge of Northern South America is located in a tectonic convergence zone involving at least three plates, the Nazca and Caribbean oceanic plates, and the continental South American plate (SAP) (Fig. 1). The Nazca Plate (NP), located to the west, is subducting eastward beneath the SAP at a rate of 5–7 cm/yr. The Caribbean Plate (CP), located to the north, is subducting east-south-eastward beneath the SAP at a lower rate of 13 mm/yr (Mora-Páez et al., 2019), possibly due to its buoyancy (Pennington, 1981). Additionally, the Coiba and Malpelo microplates have been reported in the region due to independent lithospheric behavior from the NP (e.g., Adamek et al., 1988; Hardy, 1991; Zhang et al., 2017).

The NAB, a deformable segment of the continental plate, is moving towards the northeast at a rate of 8.6 mm/yr relative to the SAP (Mora-Páez et al. 2019). Furthermore, an exotic terrane with the CP called the Chocó Block (Duque-Caro, 1990), or Panamá-Chocó Arc

(Redwood, 2019) or Panamá-Chocó Block (Suter et al., 2008), is colliding with but does not subduct beneath South America due to its buoyancy. The PCB was accreted to Northwestern South America during the Middle Miocene (Duque-Caro, 1990) or possibly before (Barat et al., 2014; Montes et al., 2012, 2015; León et al., 2018), and it still collides with the SAP at a rate of 15–18 mm/yr relative to stable SAP (Mora-Páez et al., 2019). Kellogg et al. (1995) based on GPS observations has already considered a rigid collision of the PCB against the North Andean region. It has been proposed to act as a rigid indenter (Trenkamp et al., 2002; Suter et al., 2008).

Because of the convergence of these three major plates and blocks, the northwestern Andes are subject to a transpressive tectonic regime, and the PCB – NAB interaction is characterized by a NW – SE compression that results in left lateral slip of the UFZ (Cortés and Angelier, 2005) (Fig. 1). This interpretation is still under debate, as some authors have proposed that the PCB represents a segment of the CP that subducts beneath the SAP (Taboada et al., 2000).

* Corresponding author.

E-mail addresses: danmartinezjar@geociencias.unam.mx (D. Martínez-Jaramillo), gaprietogo@unal.edu.co (G.A. Prieto).

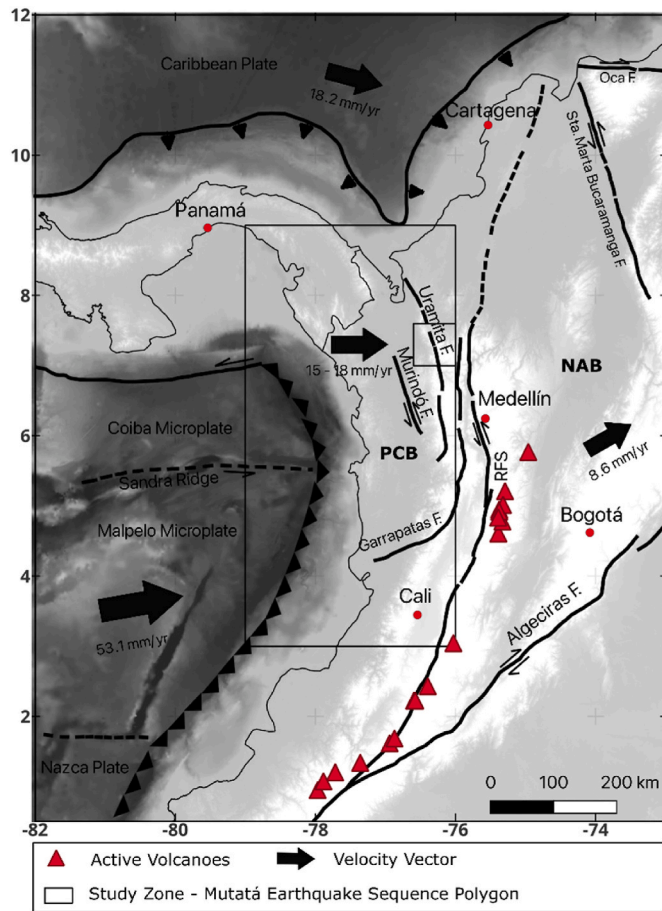


Fig. 1. Northwestern Andes main tectonic features. PCB = Panamá Chocó Block, NAB = North Andean block, RFS = Romeral Fault System. Modified from Mosquera-Machado et al. (2009) and Mora-Paéz et al. (2019).

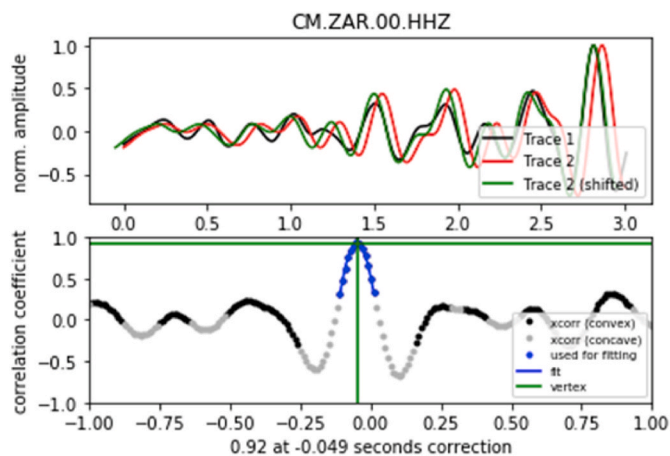


Fig. 2. Two earthquake waveform traces registered at the ZAR station were compared and shifted to get the precise correlation coefficient and the time-shifted to apply times corrections.

In general, the crustal deformation and seismogenesis of the Northwestern Andes can be explained as a result of interaction between these plates and blocks (Arcila and Muñoz Martín, 2020). We aim to frame the PCB in the local geodynamic context.

Crustal seismicity is present along the western SAP continental margin as upper plate response to the NP subduction, and uplift related to the Northern Andes. However, seismicity increases north of 4°N due

to the ongoing collision of the PCB against western Colombia and reaches its highest rate at 7°N close to the UFZ and Murindó fault. This region, called the MSC (Dionicio and Sánchez, 2012) has the highest rate of crustal activity in Colombia caused by the squeezing of the zone between the PCB and the Antioquean batholith (Tary et al., 2022). Several significant earthquakes have been reported in the zone as 1952-10-14, Mw = 5.9, Mutatá; 1977-08-30, Mw = 6.5, Apartadó; 1992-10-18 Mw = 7.1, Murindó (Servicio Geológico Colombiano (SGC) historical catalog), and 2016-09-14, Mw = 6.4, Mutatá earthquake analyzed here in detail later in the text.

Intermediate depth seismicity is observed in the region featuring distinct Wadati-Benioff zones, which are the result of multiple subducted slabs under the Northern Andes (Pennington, 1981; Freymueller et al., 1993; Taboada et al., 2000; Vargas and Mann, 2013; Yarcé et al., 2014; Syracuse et al., 2016; Chiarabba et al., 2016; Sun et al., 2022). These earthquakes also have significant implications for hazards in the region (e.g., 2012-09-30, Z = 171 km, Mw = 7.1, La Vega, Cauca; and 2013-02-09, Z = 153 km, Mw = 7.3, Guaitarilla, Nariño, reported by SGC).

For the western border of the Andes, there is a clear Wadati – Benioff zone, but north of about 5.7°N latitude, there is a seismicity gap at those depths and no clear intermediate depth seismicity north of there, possibly due to a slab tear (Caldas Tear) between NP and CP (Vargas and Mann, 2013); or where the NP changes subduction angle from normal to the south to flat subduction to the north (Chiarabba et al., 2016; Wagner et al., 2017; Syracuse et al., 2016). Other possible explanations have also been proposed related to the subduction of the young and warm slab structure of the Coiba microplate (Sun et al., 2022) or its southern boundary, Sandra Rift (Martínez-Jaramillo, 2016; Fandiño, 2020).

In this study, we improve the location of both, shallow and intermediate-depth earthquakes to interpret the crustal structure and subduction process related to the tectonic setting in Northwestern South America.

2. Local geology

The configuration of the western border of the northwestern SAP is a result of multiple accretion events of allochthonous oceanic plateaus and island arcs to the continental margin (Restrepo and Toussaint, 1988; Moreno-Sánchez and Pardo-Trujillo, 2002; Cediel et al., 2003; Spikings et al., 2015). Firstly, it began with the migration of CP from a Pacific origin to the northeast, where the junction of the Caribbean Large Igneous Province (CLIP) to South America happened during the Campanian (Villagómez and Spikings, 2013; Botero-García et al., 2023). Kerr et al. (1997) provided detailed geochemical and petrological evidence supporting the obduction and imbrication of segments of the Caribbean Large Late Cretaceous Oceanic Plate against SAP, forming a series of mafic terranes composed of picrites, basalts, and dolerites that make up western Colombia.

Additionally, another oceanic affinity terrain, the PCB, was accreted to western Colombia (Duque-Caro, 1990). The PCB is a volcano-plutonic island arc with oceanic affinity related to the CLIP on the western edge of the CP (Redwood, 2019). This block is considered a rigid indenter (Suter et al., 2008) that collides with the Caribbean-affinity western edge of South America in the Middle Miocene or earlier, based on provenance analysis, biostratigraphy, and stratigraphic relationship (Duque-Caro, 1990; Barat et al., 2014; Montes et al., 2012; 2015; León et al., 2018).

3. Methods

To obtain the new high-resolution catalog with a homogeneous relocation technique, we initiated the process using Source-Specific Station Terms (SSST) (Richards-Dinger and Shearer, 2000; Lin and Shearer, 2005) and Shrinking-Box SSST (Lin and Shearer, 2005) to reduce the bias effects of the assumed 1D velocity model, considering

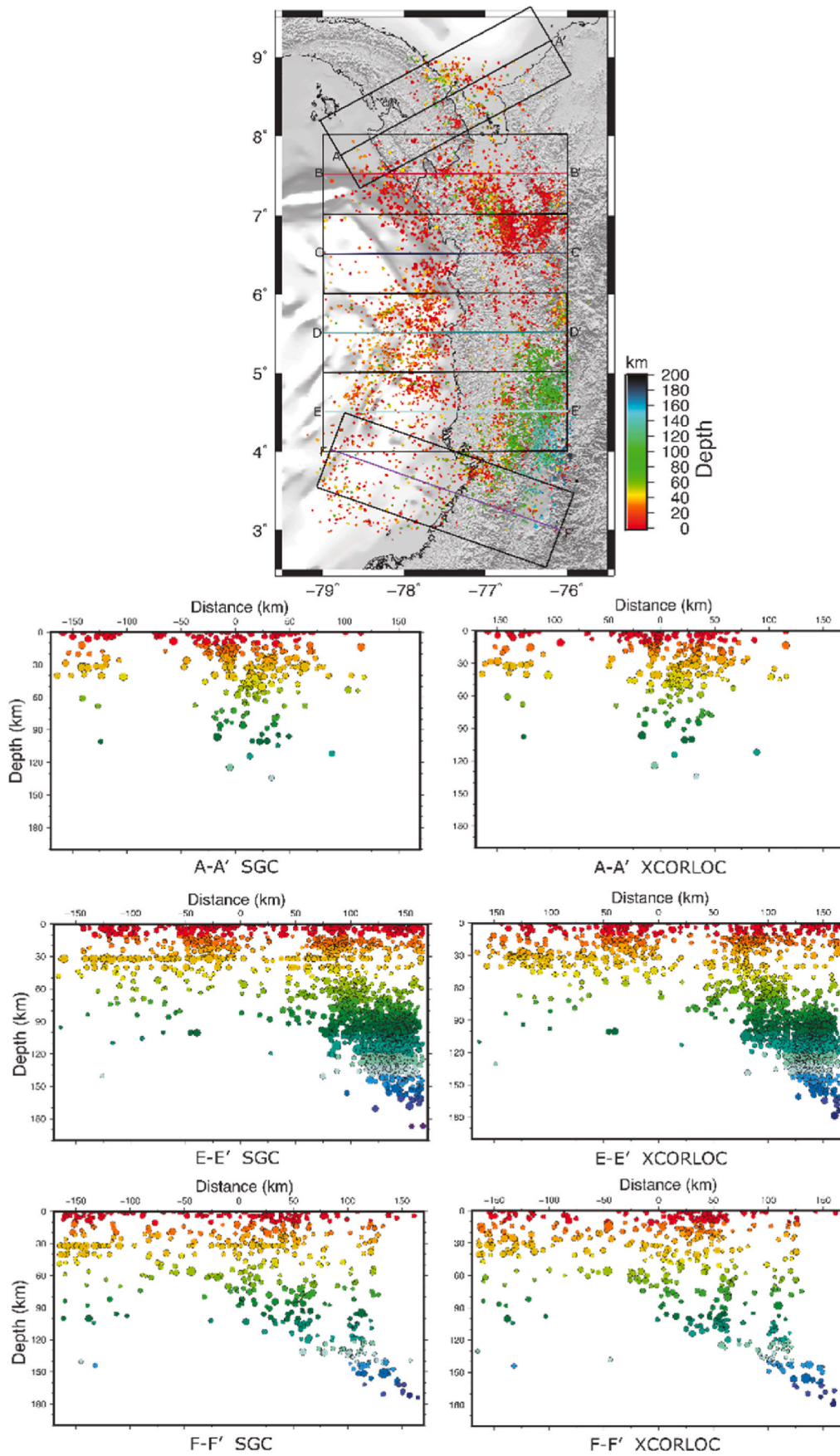


Fig. 3. Earthquakes profiles in western Colombia. Profiles A-A' are related to the Caribbean plate while E-E' and F-F' are to Nazca plate.

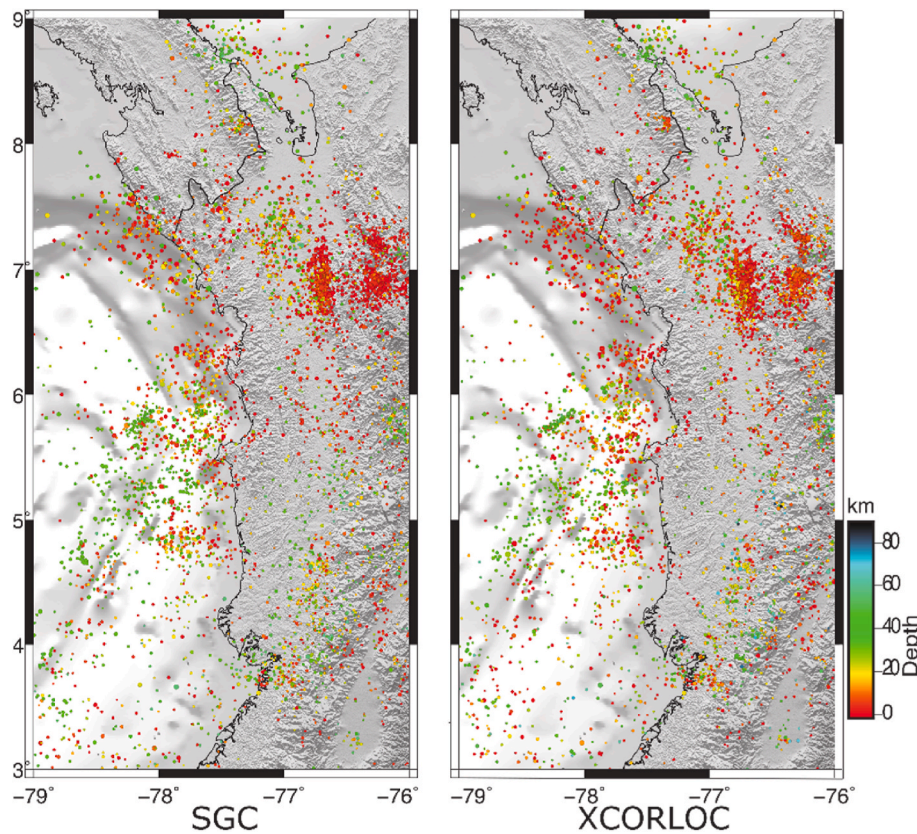


Fig. 4. Comparison between shallow seismicity from original (SGC) and relocated catalog (XCORLOC).

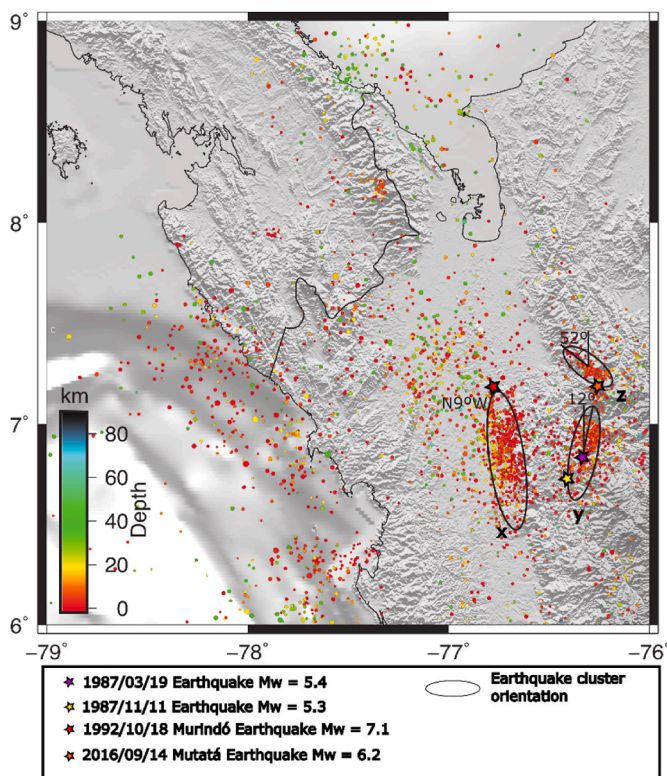


Fig. 5. North zone crustal seismicity clusters x, y and z and large events.

the complex geology and irregular layers in western Colombia.

Additionally, we used waveform cross-correlations between pairs of events to improve the relative location by measuring a more precise delay time between them and improving phase picking (Fig. 2) (Lin, 2018). This method uses small shifts in arrival times to precisely constrain the relative locations of nearby events (Husen and Hardebeck, 2010). The advantage of using cross-correlations is that the relative arrival times between two earthquakes recorded at the same station are based on the entire waveforms and their similarity. This has been shown to improve relative location and better delineate linear features such as active faults not easily detected using standard location methods (e.g., Schaff and Waldhauser, 2005; Valoroso et al., 2013; Shearer, 1997; Shearer et al., 2005). Furthermore, we applied the solution for the Least Absolute Deviation (L1) proposed by Shearer (1997) to reduce the bias of possible outliers. We refer the reader to Lin and Shearer (2005), where the SSST and Shrinking Box-SSST methods are described in detail.

We separated shallow seismicity (depth <60 km, approximately 5200 events) and intermediate-depth seismicity (depth >60 km, nearly 2200 events) for cross-correlation of pairs of events at the same stations. Additionally, we utilized a smaller dataset to define optimal parameters, subsequently applied to the entire catalog. The smaller dataset comprised the Mutatá earthquake (2016-09-14 01:58 UTC, Mw = 6.2), its main aftershock (2016-09-14, 06:46 UTC, Mw = 4.7), and 170 aftershocks located in the study area. We tested with different filters for the cross-correlations including 1–5 Hz, 0.5–3 Hz, and 0.5–5 Hz, using 2.0 s long time windows around the P and S arrival times. Our findings indicate that the 1–5 Hz filter produced superior results for our dataset. The original data, provided and processed by the SGC, included the earthquake source parameters (latitude, longitude, depth, and origin time) and the source-receivers arrival times of the P and S waves.

To elucidate the linear features observed in the relocated catalog and associate them with possible faults, we used the publication of Paris et al. (2000). Subsequently, we compared the patterns of crustal

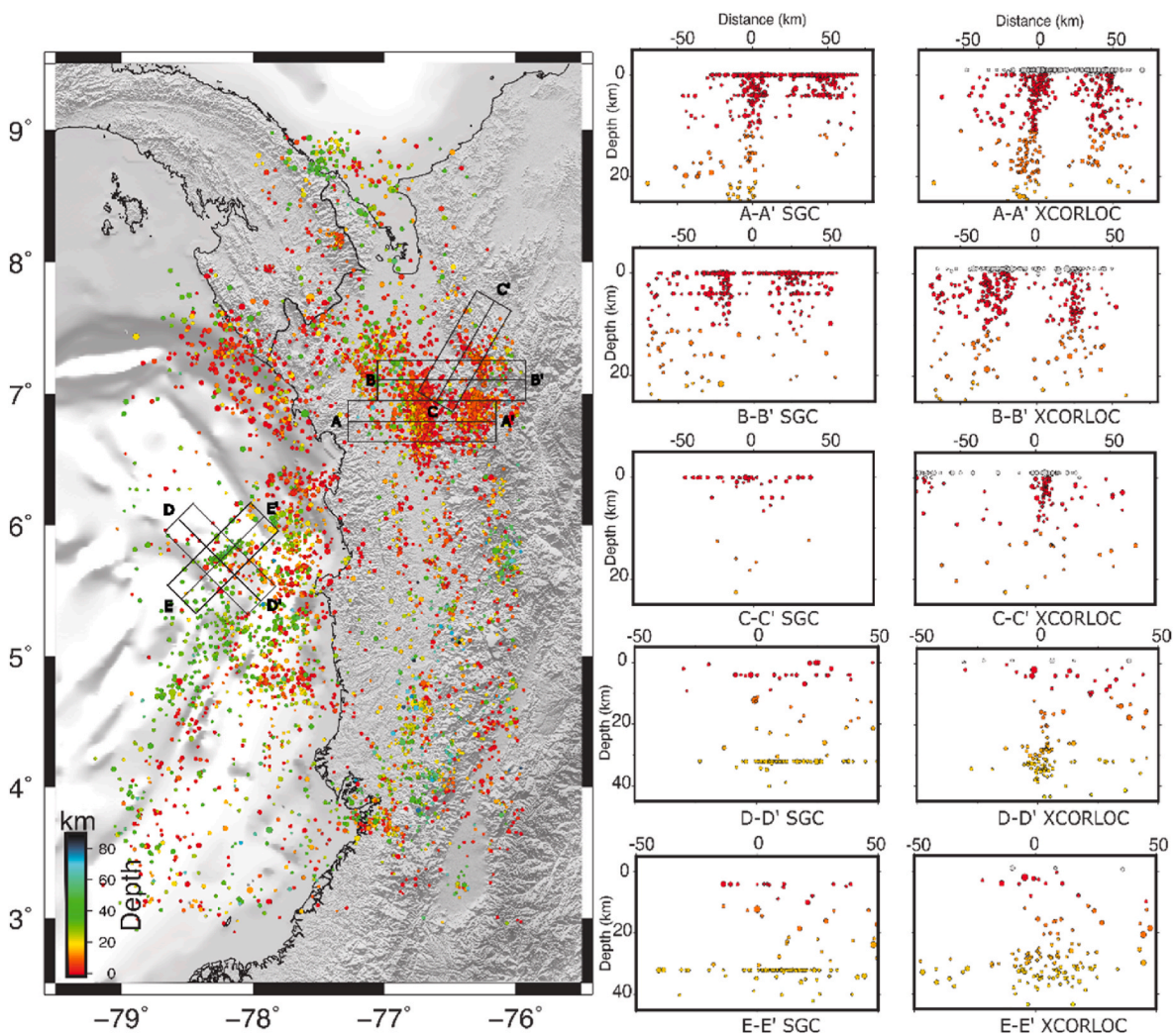


Fig. 6. Crustal seismicity profiles, A-A', B-B', and C-C' correspond to Murindó Seismic Cluster while D-D' and E-E' to offshore seismicity.

seismicity presented here with previously described fault geometry.

We used focal mechanisms from the Global Centroid Moment Tensor (GCMT) catalog (Ekström et al., 2012) to interpret seismicity slip in the zone and the compressional stress axis from Cortés and Angelier (2005) to project it onto faults and interpret its slip.

4. Results and discussion

4.1. New earthquake catalog

The seismicity of the entire region is plotted in Fig. 3, where the right side showcases the newly relocated catalog and the left side displays the original catalog. Our analysis commences with a description of intermediate-depth seismicity, followed by an examination of patterns associated with shallow earthquakes focusing on the MSC to elucidate the seismogenic behavior of the crust.

4.2. Intermediate-depth seismicity: subducting slabs

Profile A-A' in Fig. 3 presents a SW-NE cross-section, revealing intermediate-depth seismicity indicative of a Wadati-Benioff zone beneath Panamá, dipping southwestward. These observations provide further evidence of an active subduction of the CP beneath Panamá (Camacho et al., 2010). Additionally, a recent $M_w = 6.5$ (2023-05-25) earthquake in the region may shed additional light on the subduction process if it does indeed exist.

Fig. 3 profiles E-E' and F-F' show the Wadati-Benioff zones associated with the subduction of the NP (new data proposes the Malpelo microplate) beneath South America and a region known as Cauca Cluster (Chang et al., 2017, 2019). The E-E' profile shows a very productive subduction segment dipping eastward. The seismicity seems to occur over a wide range of depths along the Wadati-Benioff zone, and no clear double-seismic zone is evident (Florez and Prieto, 2019).

The F-F' profile exhibits a well-defined Wadati-Benioff zone, accompanied by seismicity above the subducted slab in the mantle wedge, extending down to 135 km depth in a sub-vertical direction. At least three of these seismicity patterns originate from the subducted slab at 75, 105 and, 135 km depths, ascending until they become indistinguishable from crustal seismicity. These structures, sometimes referred to as mantle-wedge earthquakes (Halpaap et al., 2019; Angiboust et al., 2021) have been reported in this region, featuring a finger-shaped zone of seismicity above the subducting slab (Chang et al., 2017, 2019). This type of seismicity may be associated with the upward migration of melt (Špičák et al., 2004) or fluid (Špičák et al., 2009) products of dehydration in the subducting plate (Halpaap et al., 2019). Such a process likely modifies the physical properties in the upper mantle, probably causing brittle fracturing instead of ductile deformation (White et al., 2019).

The easternmost segment of the finger-shaped seismicity in the F-F' profile is located in proximity to the Nevado del Huila volcano, indicating a plausible fluid migration path from the NP (or Malpelo microplate) through the upper mantle. This interaction with the base of the crust gives rise to melt, which, in turn, feeds the volcano. Additional

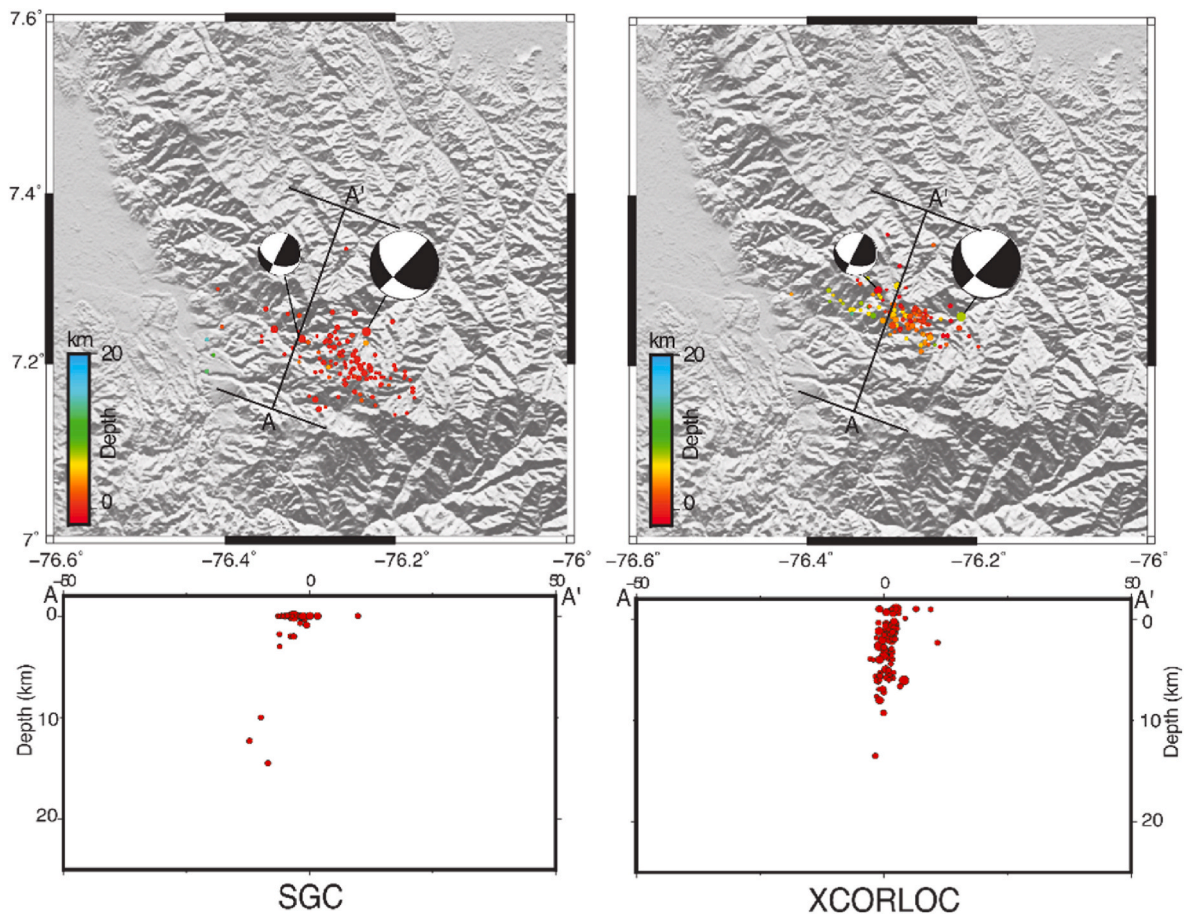


Fig. 7. Mutatá Earthquake Sequence (2016-09-14) locations and focal mechanisms reported by SGC.

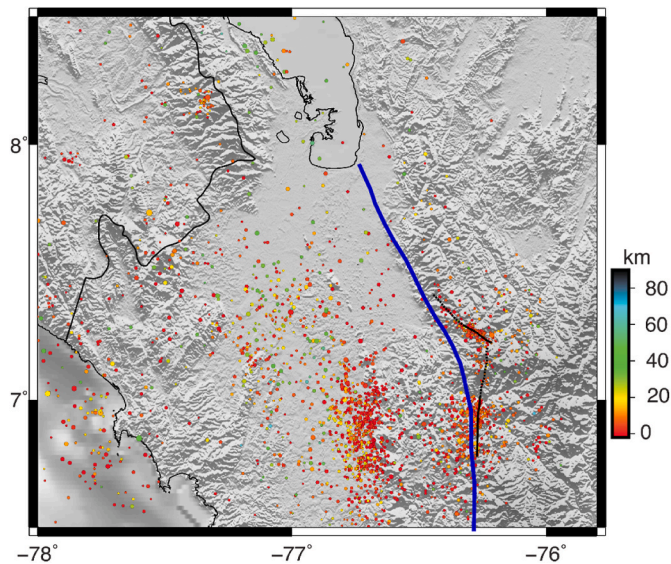


Fig. 8. Previous UFZ highlighted and focal mechanisms of the Mutatá sequence. The blue line is the limit between PCB and NAB (León et al., 2018) and the dotted line is our refined limit.

profiles (C-C', D-D', and E-E') can be referenced in the supplementary material.

4.3. Shallow seismicity: crustal seismogenic behavior

In Fig. 4 we present the shallow seismicity of the region, featuring the relocated catalog to the right and the original catalog on the left.

The most active clustered seismicity in the region within the MSC is concentrated around 7°N and 76°W – 77°W. We assert that our relocated catalog highlights the linear trends in seismicity, evident in Fig. 5 within the ellipses x, y, and z, which represent three distinct seismicity clusters. Fig. 6 provides a depth distribution of these clusters, with Profiles A-A' and B-B' showing the x and y seismicity trends, and Profile C-C' portraying the z seismicity trend.

The x, y, and z seismicity trends match with the Murindó, Murri and Mutatá faults reported by Paris et al. (2000), respectively. However, we use the classical nomenclature of Duque-Caro (1990), who first described the PCB as delimited by the UFZ. Hence, in addition to detailed geological determinations of the limit (Pardo-Trujillo et al., 2020; León et al., 2018), we constrain the main crustal deformation trends, which we associate with this limit as the couple of Murri and Mutatá faults. Subsequently, these will be referred to as the central segment of the UFZ (y) and the northern segment of the UFZ (z).

For the Murindó fault, Paris et al. (2000) reported a strike of $N12.6^\circ W \pm 6$, coinciding with the orientation of the x trend ($N9^\circ W$), as illustrated on the left side of Profiles A-A' and B-B' in Fig. 6. Regarding the central segment of the UFZ, Paris et al. (2000) reported a strike of $N1.4^\circ E \pm 6$ while our findings indicate the y trend oriented $N12^\circ E$ (Fig. 5 and right side of profiles A-A' and B-B' in Fig. 6). The z trend is oriented $S52^\circ E$ in Fig. 6, while Paris et al. (2000) report an orientation of

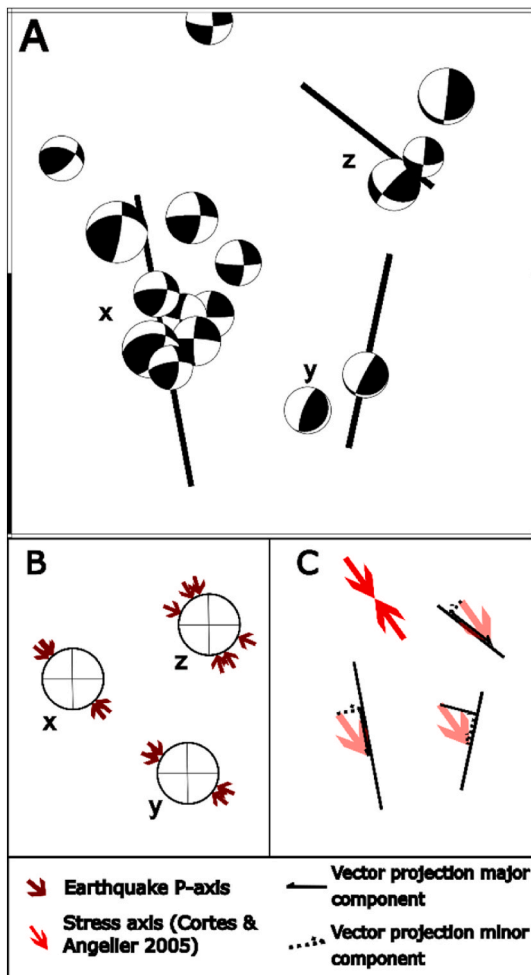


Fig. 9. A: Focal Mechanisms of earthquakes ($M_w > 5.0$) from GCMT Catalog. Clustered seismicity: x is the cluster comprising the Murindó Sequence 1992-10-17 $M_w = 6.6$ and 1992-10-18 $M_w = 7.1$. z is the cluster of the Mutatá Sequence (2016-09-14) and the Apartadó Earthquake $M_w = 6.5$ (1977-08-30). y is the cluster comprises 1987-03-19 $M_w = 5.4$ earthquake and 1987-11-11 $M_w = 5.3$ earthquake. B: Earthquakes P-axis of clustered seismicity. C: Cortés and Angelier (2005) crustal stress compression axis ($N324^\circ E$) and its projection onto faults.

$S33.6^\circ E \pm 11^\circ$. This alignment is also evident in the profile C-C' in Fig. 6, where the seismicity dips 80° to the southwest.

Selected offshore profiles D-D' and E-E' in Fig. 5 show the distribution of seismicity on the Pacific coast with an NE-oriented alignment (around $N60^\circ E$). The two profiles are perpendicular to each other, with D-D' oriented across seismicity lineation, revealing clustering at 32 km depth. Meanwhile, the E-E' profile is along the seismicity orientation. The closest structure reported to this seismicity is Sandra Rift (Lonsdale, 2005).

Table 1

Major earthquakes in the region $M_w > 5$ for each ellipse, location from ISC-EHB Catalog (Weston et al., 2018), and focal mechanisms from GCMT (Ekström et al., 2012). Mutatá earthquake and the larger aftershock from SGC.

Ellipse	Date	Strike	Dip	Rake	P-axis strike	P-axis plunge	Lat	Lon	Depth	M_w
z	1977-08-30	101	17	-175	293	44	7.339	-76.166	24.1	6.5
y	1987-03-19	38	17	106	295	29	6.737	76.432	10	5.4
y	1987-11-11	92	13	154	308	38	6.805	76.321	11.8	5.3
x	1992-10-17	28	60	55	142	8	6.854	-76.733	12.8	6.6
x	1992-10-18	9	81	46	132	23	7.079	76.798	21.1	7.1
z	2016-09-14	137	51	-168	351	34	7.238	76.234	22	6.2
z	2016-09-14	113	43	176	329	29	7.230	76.31	24	4.7

4.4. Mutatá earthquake sequence

The relocated distribution of the Mutatá earthquake sequence (2016-09-14, $M_w = 6.2$), including the focal mechanisms of the main and larger aftershock (strike = 137° , dip = 51° , rake = -168° ; strike = 113° , dip = 43° , rake = 176° , respectively, as reported by SGC; see Fig. 7), aligns with the z ellipses orientation, corresponding to the north segment of the UFZ. Both major earthquakes in the 2016-09-14 sequence indicate dextral strike-slip movement (Martínez-Jaramillo, 2020; Tary et al., 2022).

The crustal seismicity trends ellipses x and y show an abrupt change in strike between them. On the other hand, consistent depth in the majority of earthquakes suggests that the seismogenic thickness of the crust in the MSC zone is approximately 15–18 km.

4.5. The kinematics of the PCB - NAB border

We detailed defined the boundary between PCB and NAB. The previously reported was plotted and compared with our interpretation in Fig. 8. In estimating the coseismic faulting slip within the zone, the focal mechanisms of major earthquakes with a magnitude greater than 5 from the GCMT (Ekström et al., 2012) were plotted in Fig. 9 A and relevant for each ellipse compiled in Table 1. Subsequently, the P-axis for major events was plotted (Fig. 9 B), and the stress regime axis $N324^\circ E$ for the zone from Cortés and Angelier (2005) was incorporated to project onto faults (Fig. 9 C).

For instance, the projection of the regional compressional axis onto the x trend results in a main parallel and minor orthogonal component (Fig. 9 C). Similarly, events associated with the Murindó fault show obliquity with major sinistral and minor reverse components in the focal mechanisms.

The projected compressional axis onto the central segment of our representation of the Uramita fault (y trend) suggests an orthogonal main component, in agreement with the observed faulting in the reverse-predominant focal mechanisms indicated around y in Fig. 9 A (1987-03-19 and 1987-11-11 events).

In the context of the north segment of the Uramita fault, the projected main stress onto the z trend indicates a main parallel and minor orthogonal component, in agreement with a dextral lateral slip with a minor reverse component (Fig. 9 z), contributing to the Mutatá earthquake sequence. In general, the projection of regional stress onto faults reveals the slip pattern observed on earthquakes through focal mechanisms.

Tary et al. (2022) support the idea that the MSC experiences squeezing between the PCB and the Antioquean batholith. However, Cortés and Angelier (2005) pointed out that the compressional stress in the zone is likely primarily influenced by the CP. These results are in agreement with the last two sentences; the crust here is being compressed under the influence of the PCB and the Antioquean batholith, and also the CP is actively pushing the northern portion of the crust southeastward (for example the San Jacinto Block from Jarrin et al. (2023) could be the portion of the crust delimited to the south by the north segment of the UFZ), influencing the crustal behavior towards the compressional regime, which we represent in Fig. 10.

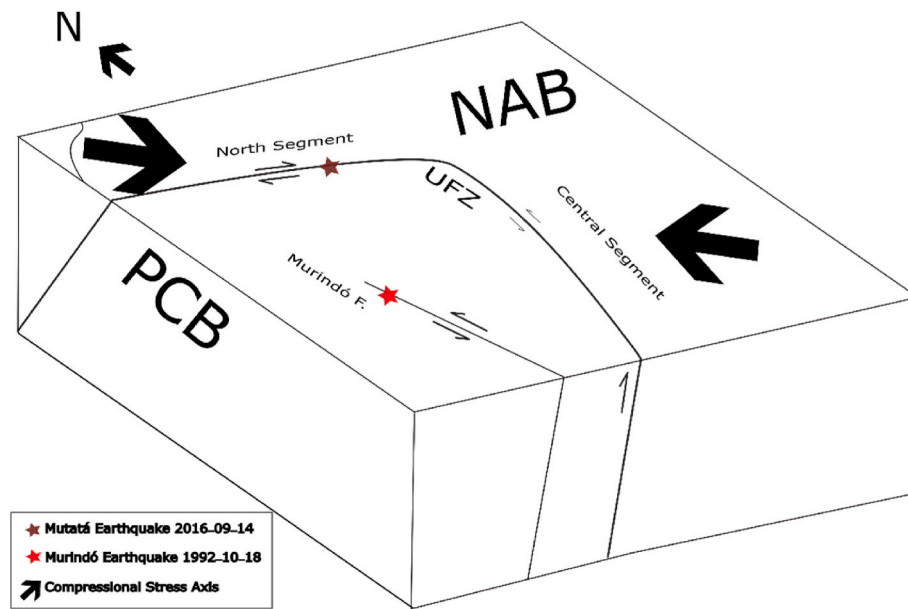


Fig. 10. Interpretation of block borders and major earthquakes from Crustal Sources NAB = North Andean block, UFZ = Uramita Fault Zone, PCB Panamá-Chocó Block.

The northeastern edge of the MSC, represented by the UFZ, serves as the limit of the PCB and NAB. To the west, the behavior of the Murindó fault is interpreted as internal deformation of the PCB, responding to the compressional stress setting in the crust. This adjustment results in the release of a high rate of coseismic elastic strain energy, exemplified by events such as the one on 1992-10-18 and the most active crustal seismicity in the northwestern Andes.

5. Conclusions

The crustal continental seismicity observed in this region is the product of a complex deformation zone resulting from the collision of blocks with oceanic affinity. The MSC is a highly active region for crustal earthquakes, situated in the northeastern corner of the PCB.

The seismicity patterns suggest that the UFZ can be interpreted as two segments with distinct orientations. This mark changes in the coseismic faulting slip of each segment under the compressional NW-SE stress regime. The northern segment aligns to S52°E, exhibiting mainly dextral-lateral slip, while the central segment trends strikes N12°E, showing predominantly reverse slip.

The slip in the Murindó fault is characterized by sinistral-strike slip, primarily resulting from the internal deformation of the block under the NW-SE compressional axis. This deformation is notably influenced by the southeastward pushing of the CP to NAB and the convergence between the PCB and NAB, as observed in the general dynamics observed in the MSC.

Offshore on the Colombian coast at 5.7°N, a seismicity trend pointing northeast is identified at 32 km depth, possibly associated with Sandra Rift.

The subduction of the Malpelo microplate reveals a complex pattern of intermediate-depth seismicity, particularly in the highly concentrated Cauca Cluster. This cluster extends beyond typical intraplate subduction earthquakes, encompassing mantle wedge cumulus formations centered at 4.60°N, 76.25° W, and 110 km depth.

South of 4°N, at least three mantle wedge sub-vertical seismicity channels extend from the subducted slab at 75, 105, and 135 km depth upward to the crust. This seismicity may indicate fluid migration, potentially altering the physical properties of the mantle and triggering earthquakes at these depths.

Data and resources

Waveforms, seismic event locations, and focal mechanisms used in this study were provided by Servicio Geológico Colombiano (SGC). Waveforms can be downloaded from: <http://sismo.sgc.gov.co:8080/fdsnws/dataselect/1/builder>, location parameters from: <http://bdrsnc.sgc.gov.co/paginas1/catalogo/index.php>. Focal Mechanism can be consulted at http://bdrsnc.sgc.gov.co/sismologia1/sismologia/focal_seiscomp_3/index.html and <https://www.globalcmt.org/CMT5/arch.html>. The historical seismicity parameters can be consulted at <https://sish.sgc.gov.co/visor/>. You can obtain the new catalog by contacting the authors. The main software packages used here were Obspy (Beyreuther et al., 2010) for processing seismological data, XCORLOC (Lin, 2018) for earthquake location, and GMT (Wessel et al., 2017) for plotting images.

CRediT authorship contribution statement

Daniel Martínez-Jaramillo: Writing - original draft, Formal analysis, Conceptualization. **Germán A. Prieto:** Writing - review & editing, Supervision, Formal analysis, Conceptualization.

Declaration of competing interest

The authors declare that they have no known competing financial interests or personal relationships that could have appeared to influence the work reported in this paper.

Data availability

Data will be made available on request.

Acknowledges

Daniel Martínez-Jaramillo is a doctoral student from Programa de Doctorado en Ciencias de la Tierra, Universidad Nacional Autónoma de México (UNAM) and received fellowship 1184401 from CONAHCYT. We want to express our gratitude to Jeffrey Freymueller and the anonymous reviewer who significantly contributed to improving this paper.

Appendix A. Supplementary data

Supplementary data to this article can be found online at <https://doi.org/10.1016/j.jsames.2023.104761>.

References

- Adamek, S., Frohlich, C., Pennington, W.D., 1988. Seismicity of the Caribbean-Nazca boundary: constraints on microplate tectonics of the Panama region. *J. Geophys. Res. Solid Earth* 93 (B3), 2053–2075.
- Angiboust, S., Muñoz-Montecinos, J., Cambeses, A., Raimondo, T., Deldicque, D., Garcia-Casco, A., 2021. Jolts in the Jade factory: a route for subduction fluids and their implications for mantle wedge seismicity. *Earth Sci. Rev.* 220, 103720.
- Arcila, M.M., Muñoz Martín, Alfonso, 2020. Integrated perspective of the present-day stress and strain regime in Colombia from analysis of earthquake focal mechanisms and geodetic data. In: *The Geology of Colombia. Publicaciones Geológicas Especiales*, vol. 4. Servicio Geológico Colombiano, Bogotá (Colombia), pp. 1–21, 38.
- Barat, F., de Lépinay, B.M., Sosson, M., Müller, C., Baumgartner, P.O., Baumgartner-Mora, C., 2014. Transition from the farallon plate subduction to the collision between south and Central America: geological evolution of the Panama isthmus. *Tectonophysics* 622, 145–167.
- Beyreuther, M., Barsch, R., Krischer, L., Megies, T., Behr, Y., Wassermann, J., 2010. ObsPy: a Python toolbox for seismology. *Seismol. Res. Lett.* 81 (3), 530–533.
- Botero-García, M., Vinasco, C.J., Restrepo-Moreno, S.A., Foster, D.A., Kamenov, G.D., 2023. Caribbean–South America interactions since the Late Cretaceous: insights from zircon U–Pb and Lu–Hf isotopic data in sedimentary sequences of the northwestern Andes. *J. S. Am. Earth Sci.* 123, 104231.
- Camacho, E., Hutton, W., Pacheco, J.F., 2010. A new look at evidence for a Wadati–Benioff zone and active convergence at the north Panama deformed belt. *Bull. Seismol. Soc. Am.* 100 (1), 343–348.
- Cediel, F., Shaw, R.P., Cáceres, C., 2003. Tectonic Assembly of the Northern Andean Block.
- Chang, Y., Warren, L.M., Prieto, G.A., 2017. Precise locations for intermediate-depth earthquakes in the Cauca cluster, Colombia. *Bull. Seismol. Soc. Am.* 107 (6), 2649–2663.
- Chang, Y., Warren, L.M., Zhu, L., Prieto, G.A., 2019. Earthquake focal mechanisms and stress field for the intermediate-depth Cauca cluster, Colombia. *J. Geophys. Res. Solid Earth* 124 (1), 822–836.
- Chiarabba, C., De Gori, P., Faccenna, C., Speranza, F., Seccia, D., Dionicio, V., Prieto, G. A., 2016. Subduction system and flat slab beneath the Eastern Cordillera of Colombia. *G-cubed* 17 (1), 16–27.
- Cortés, M., Angelier, J., 2005. Current states of stress in the northern Andes as indicated by focal mechanisms of earthquakes. *Tectonophysics* 403 (1–4), 29–58.
- Dionicio, V., Sánchez, J.J., 2012. Mapping of b-values, earthquake relocation, and Coulomb stress changes during 1992–2007 in the Murindó seismic zone, Colombia. *J. Seismol.* 16, 375–387.
- Duque-Caro, H., 1990. The Choco Block in the northwestern corner of South America: structural, tectonostratigraphic, and paleogeographic implications. *J. S. Am. Earth Sci.* 3 (1), 71–84.
- Ekström, G., Nettles, M., Dziewoński, A.M., 2012. The global CMT project 2004–2010: Centroid-moment tensors for 13,017 earthquakes. *Phys. Earth Planet. In.* 200, 1–9.
- Fandiño, J.H., 2020. Geometría de subducción de la placa de Nazca bajo el noroeste de Suramérica, a partir del análisis de microsismicidad reciente, (Master Thesis). Universidad Nacional de Colombia, Bogotá.
- Florez, M.A., Prieto, G.A., 2019. Controlling factors of seismicity and geometry in double seismic zones. *Geophys. Res. Lett.* 46 (8), 4174–4181.
- Frey Mueller, J.T., Kellogg, J.N., Vega, V., 1993. Plate motions in the north Andean region. *J. Geophys. Res. Solid Earth* 98 (B12), 21853–21863.
- Halpaap, F., Rondenay, S., Perrin, A., Goes, S., Ottemöller, L., Austrheim, H., et al., 2019. Earthquakes track subduction fluids from slab source to mantle wedge sink. *Sci. Adv.* 5 (4), eaav7369.
- Hardy, N.C., 1991. Tectonic evolution of the easternmost Panama Basin: some new data and inferences. *J. S. Am. Earth Sci.* 4 (3), 261–269.
- Husen, S., Hardebeck, J., 2010. Earthquake Location Accuracy. CORSSA.
- Jarrin, P., Nocquet, J.M., Rolandone, F., Mora-Páez, H., Mothes, P., Cisneros, D., 2023. Current motion and deformation of the Nazca Plate: new constraints from GPS measurements. *Geophys. J. Int.* 232 (2), 842–863.
- Kellogg, J.N., Vega, V., Stallings, T.C., Aiken, C.L., 1995. Tectonic Development of Panama, Costa Rica, and the Colombian Andes: Constraints from Global Positioning System Geodetic Studies and Gravity. *Special Papers-Geological Society of America*, 75–75.
- Kerr, A.C., Marriner, G.F., Tarney, J., Nivia, A., Saunders, A.D., Thirlwall, M.F., Sinton, C. W., 1997. Cretaceous Basaltic Terranes in western Colombia: elemental, chronological and Sr–Nd isotopic constraints on petrogenesis. *J. Petrol.* 38 (6), 677–702.
- León, S., Cardona, A., Parra, M., Sobel, E.R., Jaramillo, J.S., Glodny, J., et al., 2018. Transition from collisional to subduction-related regimes: an example from Neogene Panama–Nazca–South America interactions. *Tectonics* 37 (1), 119–139.
- Lin, G., 2018. The source-specific station term and waveform cross-correlation earthquake location package and its applications to California and New Zealand. *Seismol. Res. Lett.* 89 (5), 1877–1885.
- Lin, G., Shearer, P., 2005. Tests of relative earthquake location techniques using synthetic data. *J. Geophys. Res. Solid Earth* 110 (B4).
- Lonsdale, P., 2005. Creation of the cocos and Nazca plates by fission of the farallon plate. *Tectonophysics* 404 (3–4), 237–264.
- Martínez-Jaramillo, D., 2016. Geometría de la Placa de Nazca en el Pacífico colombiano a partir de datos microsísmicos (Undergraduate Thesis). Universidad de Caldas, Manizales, Colombia.
- Martínez-Jaramillo, D., 2020. Implementación del método de relocalización Source Specific Station Terms para Colombia: Aplicación para el occidente colombiano. (Master Thesis). Universidad Nacional de Colombia, Bogotá.
- Montes, C., Bayona, G., Cardona, A., Buchs, D.M., Silva, C.A., Morón, S., et al., 2012. Arc-continent collision and orocline formation: closing of the Central American seaway. *J. Geophys. Res. Solid Earth* 117 (B4).
- Montes, C., Cardona, A., Jaramillo, C., Pardo, A., Silva, J.C., Valencia, V., et al., 2015. Middle Miocene closure of the central American seaway. *Science* 348 (6231), 226–229.
- Mora-Páez, H., Kellogg, J.N., Freymueller, J.T., Mencin, D., Fernandes, R.M., Diederix, H., et al., 2019. Crustal deformation in the northern Andes–A new GPS velocity field. *J. S. Am. Earth Sci.* 89, 76–91.
- Moreno-Sánchez, M., Pardo-Trujillo, A., 2002. Historia geológica del occidente colombiano. *Geo-Eco-Trop* 26 (2), 91–113.
- Mosquera-Machado, S., Lalinde-Pulido, C., Salcedo-Hurtado, E., Michetti, A.M., 2009. Ground effects of the 18 October 1992, murindo earthquake (NW Colombia), using the environmental seismic intensity scale (ESI 2007) for the assessment of intensity. *Geological Society, London, Special Publications* 316 (1), 123–144.
- Pardo-Trujillo, A., Cardona, A., Giraldo, A.S., León, S., Vallejo, D.F., Trejos-Tamayo, R., et al., 2020. Sedimentary record of the Cretaceous–Paleocene arc–continent collision in the northwestern Colombian Andes: insights from stratigraphic and provenance constraints. *Sediment. Geol.* 401, 105627.
- Paris, G., Machette, M., Dart, R., Haller, K., 2000. Map and database of Quaternary faults and folds in Colombia and its offshore regions. US Geological Survey 61.
- Pennington, W.D., 1981. Subduction of the eastern Panama Basin and seismotectonics of northwestern South America. *J. Geophys. Res. Solid Earth* 86 (B11), 10753–10770.
- Redwood, S.D., 2019. The Geology of the Panama-Chocó Arc. *Geology and Tectonics of Northwestern South America: the Pacific-Caribbean-Andean Junction*, pp. 901–932.
- Restrepo, J.J., Toussaint, J.F., 1988. Terranes and continental accretion in the Colombian Andes. *Episodes Journal of International Geoscience* 11 (3), 189–193.
- Richards-Dinger, K.B., Shearer, P.M., 2000. Earthquake locations in southern California obtained using source-specific station terms. *J. Geophys. Res. Solid Earth* 105 (B5), 10939–10960.
- Schaff, D.P., Waldhauser, F., 2005. Waveform cross-correlation-based differential travel-time measurements at the Northern California Seismic Network. *Bull. Seismol. Soc. Am.* 95 (6), 2446–2461.
- Shearer, P.M., 1997. Improving local earthquake locations using the L1 norm and waveform cross correlation: application to the Whittier Narrows, California, aftershock sequence. *J. Geophys. Res. Solid Earth* 102 (B4), 8269–8283.
- Shearer, P., Hauksson, E., Lin, G., 2005. Southern California hypocenter relocation with waveform cross-correlation, Part 2: results using source-specific station terms and cluster analysis. *Bull. Seismol. Soc. Am.* 95 (3), 904–915.
- Špičák, A., Hanuš, V., Vaněk, J., 2004. Seismicity pattern: an indicator of source region of volcanism at convergent plate margins. *Phys. Earth Planet. In.* 141 (4), 303–326.
- Špičák, A., Vaněk, J., Hanuš, V., 2009. Seismically active column and volcanic plumbing system beneath the island arc of the Izu-Bonin subduction zone. *Geophys. J. Int.* 179 (3), 1301–1312.
- Spikings, R., Cochrane, R., Villagomez, D., Van der Lelij, R., Vallejo, C., Winkler, W., Beate, B., 2015. The geological history of Northwestern South America: from pangaean to the early collision of the caribbean large igneous Province (290–75 ma). *Gondwana Res.* 27 (1), 95–139.
- Sun, M., Bezada, M.J., Cornthwaite, J., Prieto, G.A., Niu, F., Levander, A., 2022. Overlapping slabs: untangling subduction in NW South America through finite-frequency teleseismic tomography. *Earth Planet. Sci. Lett.* 577, 117253.
- Suter, F., Sartori, M., Neuwirth, R., Gorin, G., 2008. Structural imprints at the front of the chocó-panamá indenter: field data from the North Cauca valley basin, Central Colombia. *Tectonophysics* 460 (1–4), 134–157.
- Syracuse, E.M., Maceira, M., Prieto, G.A., Zhang, H., Ammon, C.J., 2016. Multiple plates subducting beneath Colombia, as illuminated by seismicity and velocity from the joint inversion of seismic and gravity data. *Earth Planet. Sci. Lett.* 444, 139–149.
- Taboada, A., Rivera, L.A., Fuenzalida, A., Cisternas, A., Philip, H., Bijwaard, H., et al., 2000. Geodynamics of the northern Andes: subductions and intracontinental deformation (Colombia). *Tectonics* 19 (5), 787–813.
- Tary, J.B., Boada, M.J.M., Vargas, C.A., Monoga, A.M.M., Naranjo-Hernandez, D.F., Quiroga, D.E., 2022. Source characteristics of the Mw 6 Mutatá earthquake, Murindo seismic cluster, northwestern Colombia. *J. S. Am. Earth Sci.* 115, 103728.
- Trenkamp, R., Kellogg, J.N., Freymueller, J.T., Mora, H.P., 2002. Wide plate margin deformation, southern Central America and northwestern South America, CASA GPS observations. *J. S. Am. Earth Sci.* 15 (2), 157–171.
- Valoroso, L., Chiaraluce, L., Piccinini, D., Di Stefano, R., Schaff, D., Waldhauser, F., 2013. Radiography of a normal fault system by 64,000 high-precision earthquake locations: the 2009 L'Aquila (central Italy) case study. *J. Geophys. Res. Solid Earth* 118 (3), 1156–1176.
- Vargas, C.A., Mann, P., 2013. Tearing and breaking off of subducted slabs as the result of collision of the Panama Arc-Indenter with northwestern South America. *Bull. Seismol. Soc. Am.* 103 (3), 2025–2046.
- Villagómez, D., Spikings, R., 2013. Thermochronology and tectonics of the central and western cordilleras of Colombia: early cretaceous–tertiary evolution of the northern Andes. *Lithos* 160, 228–249.

- Wagner, L.S., Jaramillo, J.S., Ramírez-Hoyos, L.F., Monsalve, G., Cardona, A., Becker, T.W., 2017. Transient slab flattening beneath Colombia. *Geophys. Res. Lett.* 44 (13), 6616–6623.
- Weston, J., Engdahl, E.R., Harris, J., Di Giacomo, D., Storchak, D.A., 2018. ISC-EHB: reconstruction of a robust earthquake data set. *Geophys. J. Int.* 214 (1), 474–484.
- White, L.T., Rawlinson, N., Lister, G.S., Waldhauser, F., Hejrani, B., Thompson, D.A., et al., 2019. Earth's deepest earthquake swarms track fluid ascent beneath nascent arc volcanoes. *Earth Planet Sci. Lett.* 521, 25–36.
- Yarce, J., Monsalve, G., Becker, T.W., Cardona, A., Poveda, E., Alvira, D., Ordoñez-Carmona, O., 2014. Seismological observations in Northwestern South America: evidence for two subduction segments, contrasting crustal thicknesses and upper mantle flow. *Tectonophysics* 637, 57–67.
- Zhang, T., Gordon, R.G., Mishra, J.K., Wang, C., 2017. The Malpelo plate hypothesis and implications for nonclosure of the Cocos-Nazca-Pacific plate motion circuit. *Geophys. Res. Lett.* 44 (16), 8213–8218.